Biomaterials 31 (2010) 952–963

Contents lists available at ScienceDirect

Biomaterials

journal homepage: www.elsevier.com/locate/biomaterials

Polyethylenimine–PEG coated albumin nanoparticles for BMP-2 delivery

Sufeng Zhang [a], Cezary Kucharski [a], Michael R. Doschak [b], Walter Sebald [c], Hasan Uludağ [a,b,d,*]

[a] Department of Chemical and Materials Engineering, Faculty of Engineering, University of Alberta, Canada
[b] Faculty of Pharmacy and Pharmaceutical Sciences, University of Alberta, Canada
[c] Theodor-Boveri-Institut fur Biowissenschaften der Universität of Würzburg, Würzburg, Germany
[d] Department of Biomedical Engineering, Faculty of Medicine, University of Alberta, Edmonton, AB, Canada

ARTICLE INFO

Article history:
Received 10 August 2009
Accepted 5 October 2009
Available online 29 October 2009

Keywords:
Bone morphogenetic protein-2
Polyethylenimine–PEG
Bovine serum albumin
Nanoparticle
In vivo
Ectopic bone formation

ABSTRACT

Bone Morphogenetic Protein-2 (BMP-2) plays an important role in stimulating new bone formation, and has been utilized in clinical bone repair by implantation. In this study, we report a nanoparticulate (NP) system for BMP-2 delivery based on bovine serum albumin (BSA) NPs stabilized with a poly(ethylene glycol) modified polyethylenimine (PEI–PEG) coating. PEI–PEG with different PEG substitutions were synthesized, and the cell viability assay showed PEG substitution greatly reduced the cytotoxicity of the native PEI. Furthermore, PEI–PEG coated BSA NPs demonstrated smaller size and decreased zeta potential compared to PEI-coated NPs. The bioactivity of the encapsulated BMP-2 and the toxicity of PEI–PEG coated NPs were examined by the alkaline phosphatase (ALP) induction assay and the MTT assay, respectively, using human C2C12 cells. The results indicated that BMP-2 remained bioactive in NPs and PEI–PEG coating was advantageous in reducing the NP toxicity as compared to PEI. A 7-day pharmacokinetics study showed the BMP-2 retention in PEI–PEG coated NPs was similar to the uncoated NPs, but lower than that of the PEI-coated NPs. The osteoinductivity of BMP-2 delivered in NPs was determined by subcutaneous implantation in rats, and the results revealed that PEI–PEG coated BSA NPs induced significant *de novo* bone formation after implantation, while PEI-coated NPs demonstrated much less bone formation. We conclude that BMP-2 delivered by PEGylated PEI-coated BSA NPs displays favorable biocompatibility and promotes new bone formation after implantation.

1. Introduction

Bone morphogenetic proteins (BMPs) play an essential role in bone formation and healing. They are capable of eliciting new bone formation at ectopic and orthotopic sites in various animal models [1–8]. Due to the inherent limitations and variability of biologically derived grafts in repair of bone defects, recombinant BMPs are increasingly utilized as an alternative approach to stimulate new bone formation in clinical repair. With the validation of efficacy and safety of BMPs for bone repair [9–15], BMP-2 and BMP-7 were recently approved by FDA for spinal fusion (InFUSE® Bone Graft) and bone fracture treatment (OP-1™ Implant) in humans. Design of improved delivery systems is the next challenge for bringing more potent osteoinductive devices into clinical practice. Towards this end, biomaterials and delivery systems that can minimize the diffusion of BMP-2 away from the application site will be beneficial to obtain satisfactory bone induction, especially in higher mammals [16,17]. Preclinical studies have demonstrated a correlation between the osteoinductivity of BMP-2 and its retention in various carriers *in vivo* [18–20]. Based on these observations, it was suggested that the enhancement of protein retention in carriers [18] as well as local release [19] could potentially improve the performance of BMP-2 function at the implantation site.

The current delivery system in which BMP-2 is implanted soaked in collagen matrices, though successful in preclinical and human clinical trials, has displayed some drawbacks [21]. Initial burst release is a concern when BMP-2 is simply absorbed into carriers, which will result in less retention time period for BMP-2. By physical entrapment or covalent binding of BMP-2 to the carrier, the initial burst release could be suppressed, making it possible to prolong the local retention time and providing a sustained release. However, the difficulty in retaining the protein bioactivity limits the utilization of covalent coupling approaches to the carrier. Alternatively, bone growth factors have been physically entrapped in microparticles, nanoparticles (NPs), liposomes, hydrogels, or foams as a sustained release formulation [22]. As an efficient and

* Corresponding author. #830, Chemical & Materials Engineering Building, University of Alberta, Edmonton, Alberta, Canada T6G 2G6. Tel.: +1 780 492 0988; fax: +1 780 492 2881.
E-mail address: hasan.uludag@ualberta.ca (H. Uludağ).

0142-9612/$ – see front matter © 2009 Elsevier Ltd. All rights reserved.
doi:10.1016/j.biomaterials.2009.10.011

simple delivery system developed in 1980s, nanoparticulate delivery systems are now beginning to be explored for BMP delivery [23–28]. The nanoparticulate systems have the potential to release the entrapped drugs over a prolonged time while preserving the drug's bioactivity. Such systems can be employed for local application after surgery, as well as systemically delivered via intravascular injection [29]. We previously reported that recombinant human BMP-2 could be encapsulated in NPs constructed from serum albumin [24]. The NPs were coated with polyethylenimine (PEI) for stabilization, giving an encapsulation efficiency of >90% and BMP-2 retaining its bioactivity after release *in vitro*. The BMP-2 release from NPs was controlled by the PEI coating concentrations [24]. However, the osteoinductive activity of BMP-2 encapsulated in NPs was not readily achieved in a rat ectopic model, and we attributed this undesirable result to the toxic effect of the PEI on locally present cells [28].

Poly(ethylene glycol) (PEG) substitution on polymers is an established method for increasing polymer biocompatibility, as well as minimizing interactions among molecular and particulate species by providing steric stabilization [30,31]. In this report, we designed a new formulation of the serum albumin NPs by utilizing PEGylated PEI for NP coating in order to reduce the toxicity of coating and increase the biocompatibility of NPs under *in vivo* conditions. *N*-hydroxysuccinimidyl-poly(ethylene glycol)-maleimide (NHS-PEG-MAL) was employed as a linker to attach the PEG moiety onto the primary amines of PEI [32]. The BMP-2 encapsulated, PEI–PEG coated NPs were evaluated for BMP-2 osteoinductive activity and pharmacokinetics in a rat ectopic model by subcutaneous implantation.

2. Materials and methods

2.1. Materials

BSA, branched PEI (M_w ~ 25,000 by light scattering, M_n ~ 10,000 by gel permeation chromatography), Alkaline phosphatase (ALP) substrate p-nitrophenol phosphate (p-NPP), 2-amino-2-methyl-1-propanol (AMP), *o*-cresolphthalein, 8-hydroxyquinoline, trichloroacetic acid (TCA), picrylsulfonic acid solution (TNBS; 5% w/v) and calcium standards were obtained from Sigma–Aldrich (St. Louis, MO, USA). N-hydroxysuccinimidyl-polyethylene glycol-maleimide (NHS-PEG-MAL, 3.4 kDa) was obtained from NEKTAR (Huntsville, AL, USA). Recombinant Human BMP-2 (from *E. coli*) was prepared as described before [33]. $Na^{125}I$ (in 0.1 M NaOH) was obtained from GE Healthcare (Piscataway, NJ, USA). Metofane™ (methoxyflurane) was obtained from Janssen Inc. (Toronto, ON, Canada). Sterile saline (0.9% NaCl, non-pyrogenic) was obtained from Baxter Corporation (Toronto, ON, Canada). Fluorescein isothiocyanate (FITC) was obtained from PIERCE (Rockford, IL, USA). Hemostatic Absorbable Collagen Sponge (ACS, Helistat®) was obtained from Integra Life Sciences Corporation (Plainsboro, NJ, USA). Dulbecco's Modified Eagle Medium (DMEM), penicillin (10,000 U/mL) and streptomycin (10,000 μg/mL) were from Invitrogen (Carlsbad, CA, USA). Fetal bovine serum (FBS) was from Atlanta Biologics (Atlanta, GA, USA). Triton X-100 was obtained from Serva Feinbiochemica (Heidelberg/NY, USA). All tissue culture plasticware was from Corning (Corning, NY, USA). The Spectra/Por dialysis tubing with 12–14 kDa and 100 kDa molecular weight cut-off (MWCO) was acquired from Spectrum Laboratories Inc. (Rancho Dominguez, CA, USA). Where indicated, in-house prepared distilled/de-ionized water (ddH_2O) used for buffer preparations and dialysis was derived from a Milli-Q purification system (Millipore; Billerica, MA, USA).

2.2. Preparation of PEI–PEG conjugate [32]

The PEI–PEG conjugates were prepared by reacting PEI with desired concentrations of NHS-PEG-MAL. Briefly, the NHS-PEG-MAL was dissolved in 100 mM, pH = 7.0 phosphate buffer (see Fig. 1 for exact NHS-PEG-MAL concentrations), and PEI solution (3.6 mg/mL in 100 mM, pH = 7.0 phosphate buffer) was added to the above solution at a volume ratio of 1:1. The samples were incubated for 2.5 h at room temperature, then dialyzed (MWCO: 12–14 kDa) against 100 mM phosphate buffer (pH = 5.0, ×2), and subsequently dialyzed against ddH_2O (×2). The dialyzed buffer was exchanged every 3 h. The PEI content in PEI–PEG conjugates was determined by the copper (II)/PEI assay [34,35] and the amine content by the TNBS assay [36]. The extent of PEG substitution was determined based on the reduction of primary amine content in PEI samples as follows: 100% × [(initial amine concentration) − (final amine concentration)]/(initial amine concentration).

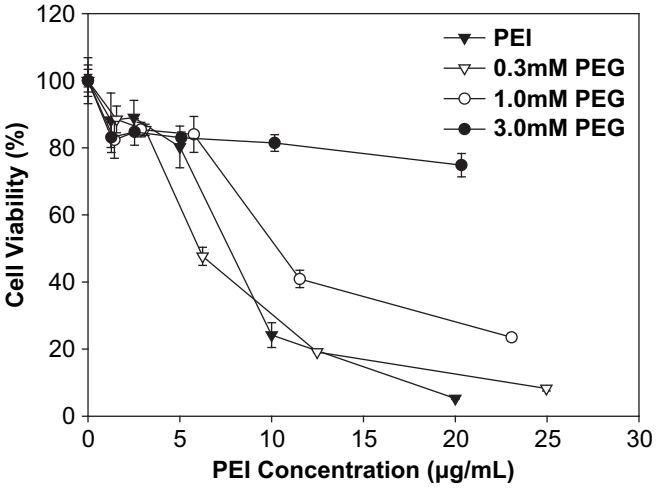

Fig. 1. Cytotoxicity of PEI and different PEI–PEG conjugates on human C2C12 cells. PEI showed strong cytotoxicity at >5 μg/mL, with only 5% cell viability being retained at 20 μg/mL. However, the PEI–PEG conjugates exhibited reduced cytotoxicity as the PEG substitution was increased.

2.3. Preparation of NPs

The details of NP preparation process were previously described [24]. Briefly, 250 μL of 10 mg/mL BSA solution was added to 250 μL of 10 mM NaCl solution (pH = 7.0) in a glass vial under constant stirring (600 rpm) at room temperature. The mixing was allowed to proceed for 15 min and 72 μL of 0.5 μg/μL BMP-2 solution (in ddH_2O) was added into this solution. This aqueous phase was then desolvated with dropwise addition of 3.0 mL of ethanol after 2 h of incubation. The mixture was stirred (600 rpm) under room temperature for another 3 h. Different concentrations of PEI–PEG (see Fig. 2 for exact concentrations) in 0.5 mM NaCl solution were added to the obtained NP suspensions by a volume ratio of 1.25:1 (polymer to NPs). The coating was allowed to proceed for 1 h on an orbital shaker (450 rpm) and the coated NPs were extensively dialyzed (MWCO: 100 kDa) against 1 mM NaCl (×3). For the bioactivity studies, the coated NPs were dialyzed (MWCO: 12–14 kDa; this was chosen to avoid the BMP-2 loss due to release during the dialysis) against phosphate buffered saline (1 × PBS, pH = 7.3, ×3), and then against DMEM with 1% penicillin/streptomycin (×1). The dialyzed buffer was exchanged every 3 h. All solutions used for NP preparation were sterilized by passing through 0.20 μm sterile filter (SARSTEDT, Aktiengesellschaft & Co., Germany) before use, and the manufacturing process was carried out under sterile conditions.

2.4. Characterization of NPs

The mean particle size and polydispersity index of the NPs were determined by dynamic light scattering at 25 °C with a Zetasizer 3000 HS (Malvern Instruments Ltd., UK) using a 633 nm He–Ne laser at a scattering angle of 90°. The surface charge of the coated and uncoated BSA NPs were investigated by measuring the electrophoretic mobility of the particles using the zeta potential modulus of the same instrument at 25 °C. The samples for measurement were prepared after appropriate dilution and suspended in 1 mM NaCl solution. The particle size and zeta potential measurements were performed in triplicate.

Atomic force microscopy (AFM) was performed on the NPs dialyzed against ddH_2O to remove salt crystals. The NP suspensions were sonicated for 5 min and then 1.5 μL of the sample was added onto the mica surface (PELCO® Mica Discs; TED PELLA, Inc.; Redding, CA, USA), and imaged under room temperature after drying [24]. MFP-3D AFM (Asylum Research, Santa Barbara, CA, USA) was used for the AFM studies, and images were analyzed by the IgorPro imaging software (version 5.04B).

2.5. Coating efficiency of NPs with FITC-PEI–PEG and FITC-PEI

The amount of polymer coated on NPs was determined by using FITC-labeled polymers for NP coating. To obtain the labeled polymer, PEI (10 mg/mL) was first reacted with FITC as described before [24] and the obtained FITC-PEI was then reacted with different concentrations of MAL-PEG-NHS as in Section 2.2. The FITC-PEI–PEG conjugates so formed were dialyzed (MWCO: 12–14 kDa) against 100 mM phosphate buffer (pH = 5.0), and subsequently against ddH_2O to remove the unreacted MAL-PEG-NHS. The NPs were prepared as described in Section 2.3 and after 1 h coating, the NPs were dialyzed (MWCO: 100 kDa) against 1 mM NaCl (×2) and ddH_2O (×1), centrifuged for 30 min at high speed (BHG Hermle Z230 M Centrifuge) to remove ethanol, free BSA and uncoated polymer, and then re-dispersed in ddH_2O. A 200 μL

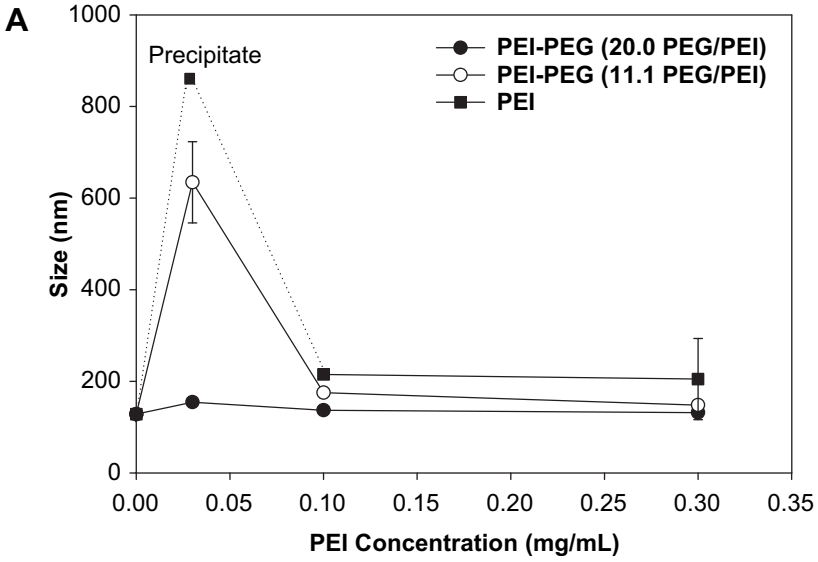

B **Polydispersity Index**

PEI concentration (mg/mL)	PEI-PEG (20.0 PEG/PEI)	PEI-PEG (11.1 PEG/PEI)	PEI
0.03	0.13 ± 0.02	1.0	N/A
0.1	0.23 ± 0.10	0.26 ± 0.03	0.27 ± 0.06
0.3	0.08 ± 0.01	0.13 ± 0.06	1.0
0	0.20 ± 0.02		

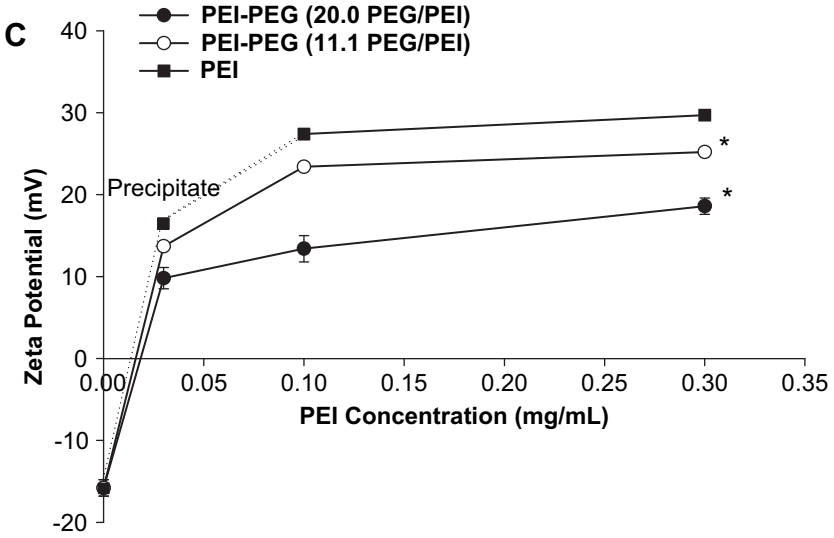

Fig. 2. The mean particle diameter **(A)**, polydispersity index **(B)** and zeta potential **(C)** of PEI–PEG and PEI-coated BSA NPs. The polymer concentrations were based on the PEI content derived from the TNBS assay. Two independent batches for each coating concentration were prepared for assessment, and each measurement was performed in triplicate runs. PEI–PEG coated BSA NPs exhibited reduced size compared with the unmodified PEI-coated NPs at the same coating concentration. The zeta potential of PEI–PEG coated NPs decreased correspondingly compared with the PEI-coated NPs (* $p < 0.001$).

aliquot in duplicate was then added to black 96-well plates (NUNC; Rochester, NY, USA) and the fluorescence (λ_{ex}: 485 nm; λ_{em}: 527 nm) was determined with a multi-well plate reader. The amount of polymer recovered in NPs was calculated based on a calibration curve generated with known concentrations of FITC-labeled polymers in ddH_2O. The coating efficiency of polymer was calculated as: 100% × {(final FITC-polymer of the pellet)/(initial FITC-polymer for coating)}.

2.6. Cytotoxicity of polymers and polymer-coated NPs

The MTT dye reduction assay was used for cytotoxicity assessment. The toxicity of PEI and PEI modified with 3 and 1 mM NHS-PEG-MAL (the PEG substitutions were 20.0 and 11.1 PEG/PEI, respectively) were examined in this study. The polymer concentrations were based on the PEI content derived from the TNBS assay. The polymers dissolved in ddH_2O solutions were added to human C2C12 cells grown in 48-well plates (in triplicate) with 0.5 mL tissue culture medium (DMEM supplemented with 10% FBS and 1% penicillin/streptomycin). After 48 h incubation, the MTT assay was performed as described before [24]. In order to determine the cytotoxicity of coated NPs, the NPs were prepared as described above, and then coated with 0, 0.03, 0.1 and 0.3 mg/mL PEI or PEI–PEG for 1 h on an orbital shaker. The samples were then dialyzed against 1 × PBS (pH = 7.3; ×3), and then DMEM with 1% penicillin/streptomycin (×1). Human C2C12 cells grown in 48-well plates were incubated for 48 h with various concentrations of NPs (in triplicate) and the MTT assay was performed as described before [24].

2.7. Assessment of ALP induction by NP formulations of BMP-2

The activity of BMP-2 in NP formulations was assessed *in vitro* by determining its ability to induce ALP activity in human C2C12 cells. The cells were grown in 48-well plates for ~24 h before the addition of NP samples. The NPs were prepared as described above, and then coated with 0, 0.03, 0.1 and 0.3 mg/mL PEI or PEI–PEG for 1 h on an orbital shaker. The samples were then dialyzed against 1 × PBS (pH = 7.3; ×3), and then DMEM with 1% penicillin/streptomycin (×1). Different volumes of NP suspensions (50 to 6.25 μL) were added to the C2C12 cells to obtain the final BMP-2 concentrations of 0.5, 0.25, 0.125 and 0.0625 μg/mL. The NPs were incubated with the cells for 72 h and a kinetic ALP assay was performed to determine the bioactivity of encapsulated BMP-2 as described before [24].

Prior to *in vivo* ectopic bone formation, the NP formulations were also tested *in vitro* for ALP activity induction. The NPs for this assay were prepared by adding 120 μL of 1.0 μg/μL BMP-2 in ddH_2O to 125 μL of 10 mg/mL BSA solution and 12.5 μL of 100 mM of NaCl in a glass vial (9.6% w/w BMP-2 in BSA), which was allowed to stir at 600 rpm for 1 h. Then, 1.0 mL of ethanol was added dropwise to the mixture, and stirred for 3 h at 600 rpm to form the NPs. The NPs were coated with 0.1 mg/mL PEI or 0.1 mg/mL PEI–PEG (20.0 PEG/PEI), which were dissolved in 0.5 mM NaCl solution. The volume ratio of NPs to polymer for coating was 1:1. The coating was allowed to proceed for 1 h on an orbital shaker. The uncoated sample was processed the same way as the coated samples, except by adding 0.5 mM NaCl solution to the NPs. The NPs were dialyzed against 1 × PBS (pH = 7.3; ×3) and DMEM (1% of penicillin/streptomycin) (×1). Different volumes of NP suspensions (giving 1.0–0.125 μg BMP-2/mL) were incubated with human C2C12 cells grown in 48-well plates and the kinetic ALP assay was performed after 72 h incubation of NPs with the cells [24].

2.8. Pharmacokinetics study

The BMP-2 in pharmacokinetics studies was labeled with ^{125}I as described in [37]. The iodinated sample was confirmed to contain <5% free ^{125}I after TCA precipitation. After iodination, 30 μL of ^{125}I-labeled BMP-2 was first diluted with 210 μL of ddH_2O, and then mixed with BSA solution for NP preparation. Briefly, 250 μL of 10 mg/mL BSA solution was added to 25 μL of 100 mM NaCl solution in a glass vial under constant stirring (600 rpm) for 15 min at room temperature. Then, 240 μL of ^{125}I-labeled BMP-2 in ddH_2O was added to this solution. This solution was desolvated with dropwise addition of 2.0 mL of ethanol and mixed (600 rpm) at room temperature for 3 h. The NPs were then coated with 0.1 mg/mL PEI or 0.1 mg/mL PEI–PEG (20.0 PEG/PEI), which were dissolved in 0.5 mM NaCl solution, at a volume ratio of 1:1. The uncoated NPs were processed under the same condition with 0.5 mM NaCl solution. The coating was allowed to proceed for 1 h on an orbital shaker and the samples were dialyzed (MWCO: 12–14 kDa) against 1 × PBS (pH = 7.3; ×2).

6–8-week-old female Sprague-Dawley rats were purchased from Biosciences (Edmonton, Alberta). The rats were acclimated for 1 week under standard laboratory conditions (23 °C, 12 h of light/dark cycle) prior to the beginning of the study. While maintained in pairs in sterilized cages, rats were provided with standard commercial rat chow, and tap water *ad libitum* for the duration of the study. All procedures involving the rats were approved by the Animal Welfare Committee at the University of Alberta (Edmonton, Alberta). The ACS used for implantation was 1 cm × 1 cm square cut from a 7.5 cm × 10 cm ACS (5.0 mm thickness). The dry sponges were then soaked for 10 min with 50 μL of the following ^{125}I-labeled samples: (1) BMP-2 in uncoated NPs, (2) BMP-2 in NPs coated with 0.1 mg/mL PEI–PEG (20.0 PEG/PEI), and (3) BMP-2 in NPs coated with 0.1 mg/mL PEI. The exact counts in the added 50 μL samples were determined by a γ-counter (Wizard 1470; Wallac, Turku, Finland) prior to implantation, and used as the total implanted BMP-2 dose. Once rats were anesthetized with inhalational Metofane™, two implants (duplicates of the same type) were implanted subcutaneously into bilateral ventral pouches in each rat. A total of twenty-seven rats were utilized for the three study groups; three rats from each group were sacrificed at 1, 4 and 7 days post-implantation, respectively. The rats were euthanized with CO_2, the implants were recovered, and the counts associated with the excised implants were quantified by using a γ-counter. The amount of BMP-2 retention, expressed as a percentage of implanted dose, was calculated as: 100% × [(recovered counts in implants)/(initial counts in implants)]. The results were summarized as mean ± SD of %implant retention of BMP-2 at each time point.

2.9. Osteoinduction in rat subcutaneous implant model

The study groups used for implantation are summarized in Table 1. The four study groups included: (1) control phosphate buffered saline; (2) uncoated BMP-2/BSA NPs; (3) 0.1 mg/mL PEI–PEG (20.0 PEG/PEI) coated BMP-2/BSA NPs; and (4) 0.1 mg/mL PEI-coated BMP-2/BSA NPs. The BMP-2 encapsulated BSA NP formulations were prepared as described in Section 2.7. This NP preparation ensured 3 μg of BMP-2 in 50 μL of NP suspension after dialysis without further concentrating the NPs. The NP samples were dialyzed against 1 × PBS (pH = 7.3, ×3). The ACS was cut into 1 cm × 1 cm × 0.5 cm pieces, to absorb 50 μL of sample for each piece. For the control ACS, 50 μL of phosphate buffered saline (1 × PBS, pH = 7.3) was absorbed into ACS (see details in Table 1), and allowed to soak for 10 min before implantation. 6–8-week-old female Sprague-Dawley rats were anesthetized with inhalational Metofane™ and two implants (duplicates of the same type) were implanted subcutaneously into bilateral ventral pouches in each rat. There were twenty-four rats utilized in this study, with each group containing 3 rats at each designated time point (10 and 16 days). Rats were euthanized with CO_2 at indicated time, and the implants were recovered, weighed before further investigation. ALP assay, micro-CT and calcium assay were carried out for the recovered implants.

Table 1
Experimental groups for osteoinduction study conducted in the rat subcutaneous implant model.

Implant set	Group	BMP-2 dose per implant (μg)	Number of animals (number of implants)	Harvest (days)	Analysis
G1	ACS	0	3 (6), 3 (6)	10, 16	weight, ALP, Ca^{2+}, Micro-CT
G2	ACS + BMP-2/BSA NP	3	3 (6), 3 (6)	10, 16	weight, ALP, Ca^{2+}, Micro-CT
G3	ACS + 0.1 mg/mL PEI–PEG coated BMP-2/BSA NP	3	3 (6), 3 (6)	10, 16	weight, ALP, Ca^{2+}, Micro-CT
G4	ACS + 0.1 mg/mL PEI-coated BMP-2/BSA NP	3	3 (6), 3 (6)	10, 16	weight, ALP, Ca^{2+}, Micro-CT

2.9.1. ALP activity in implants [38]

The explants were incubated in 2.0 mL of 1 × PBS (pH = 7.3) at 4 °C in 24-well plates overnight with gentle shaking to remove any serum contaminants. The explants were then transferred to 1.0 mL of 25 mM $NaHCO_3$ (pH = 7.4) containing 0.01% Triton X-100 for a 72 h incubation at 4 °C with gentle shaking. After 72 h, 200 μL of the sample solutions (in duplicate) from each well were placed into a 48-well-plate, and then 200 μL of p-NPP in ALP buffer (pH = 10.5, containing 0.1% of Triton X-100) was added to each extraction solution. The changes in optical density ($\lambda_{absorbance}$: 405 nm) were determined in a multi-well plate reader at an interval of 1.5 min for 8 cycles. The kinetic ALP activity was expressed as the change in optical density of the wells per minute (mABS/minute). All results were expressed as mean ± SD of duplicate wells for each recovered implant.

2.9.2. Micro-computed tomography (micro-CT) imaging of explants

After the implants were evaluated using the ALP assay, the recovered implants were imaged non-invasively at high resolution using a micro-CT imager (Skyscan-1076, Skyscan NV, Belgium). Briefly, the recovered implants were removed from the ALP buffer, and placed into 1.5 mL microcentrifuge tubes, and loaded into the imager gantry along with volumetric micro-CT calibration phantoms of known calcium phosphate density. Samples were scanned at 18 μm resolution, using a tube voltage of 48 kVp and a current of 100 μA. The X-ray beam was hardened using a 0.025 mm titanium filter in order to remove low energy photons and reduce beam hardening and edge artifacts. An imaging step of 0.35° (through 180° of rotation) was chosen in order to adequately sample the low density mineralized explants, with an image acquisition frame averaging of 3, and with a scan duration of 23 min per batch of 3 samples. The raw image data were Gaussian filtered and reconstructed using a modified Feldkamp back-projection algorithm, thresholded at an image to cross-section of 0.0004–0.0414 using vendor supplied NRecon reconstruction software (version 1.5.1). Reconstructed images for each sample were quantified for percent bone volume using vendor supplied histomorphometric image analysis software (CT-An, Skyscan NV, Belgium). Reconstructed images were rendered into 3D representations using vendor supplied CT-Vol software.

2.9.3. Assessment of calcium deposition in implants

After micro-CT evaluation, the explants were washed with 2.0 mL of 1 × PBS (pH = 7.3), and transferred to a new 24-well-plate with 1.0 mL of 0.5 N HCl per well. The explants were gently agitated for 24 h to extract the mineralized calcium. 20 μL of the dissolved calcium solution was added to 50 μL of 28 mM 8-hydroxyquinoline in 0.5% (v/v) sulfuric acid, and then 0.5 mL of 0.37 mM *o*-cresolphthalein in 1.5% (v/v) AMP was added to this solution. The absorbance was determined with a multi-well plate reader at 570 nm. A standard curve based on known concentration of calcium standards was used to convert the obtained absorbance values into calcium concentrations. The level of calcification was summarized as the mean concentration of calcium (mg/dL) ± SD of duplicate wells for each recovered implant.

2.10. Statistical analysis

All quantitative data were expressed as the mean ± standard deviation (SD). In the pharmacokinetics study, statistical analysis was performed by unpaired Student's *t*-test. In the ectopic bone formation study, statistical analysis was performed by the non-parametric Mann–Whitney–Wilcoxon test. Where indicated, statistical differences between group means were analyzed by single factor analysis of variance (ANOVA) or Kruskal–Wallis one-way analysis of variance (for non-parametric test). A value of $p < 0.05$ was considered statistically significant.

3. Results

3.1. PEG conjugation to PEI and resultant polymer cytotoxicity

By reacting the primary amines on PEI with the NHS functional group in NHS-PEG-MAL [32], a series of cationic copolymers were synthesized with 3.4 kDa PEG substitution on 25 kDa branched PEI (Scheme 1). The extent of PEG substitution was expected to be controlled by the NHS-PEG-MAL:PEI ratio during the reaction. With NHS-PEG-MAL:PEI ratios of 42:1, 14:1 and 4.2:1, the PEG substitutions obtained were 20.0, 11.1 and 4.2 PEG/PEI, respectively.

The cytotoxicity of the PEI–PEG conjugates and the unmodified PEI was determined on C2C12 cells (Fig. 1). The PEI with the lowest PEG substitution (4.2 PEG/PEI) did not significantly reduce the cytotoxicity, while the PEI with the highest PEG substitution (20.0 PEG/PEI) reduced the cytotoxicity significantly, with 78.6% cell viability at the highest concentration of 20 μg/mL tested. The moderately-modified PEI (11.1 PEG/PEI) showed some reduction in PEI toxicity. Since the PEI with the lowest PEG substitution (4.2 PEG/PEI) did not display reduced cytotoxicity, this polymer was eliminated from the subsequent studies.

3.2. Characterization of PEI–PEG coated NPs

The feasibility of PEI–PEG coating on NPs was explored next by using PEI–PEG conjugates with 20.0 and 11.1 PEG/PEI. Three polymer concentrations used for coating were 0.03, 0.1 and 0.3 mg/mL and the sizes of the NPs obtained are summarized in Fig. 2. With 0.03 mg/mL PEI, large aggregates resulted after the coating process (Fig. 2A), presumably due to the bridging flocculation among the formed particles [39]. However, PEI–PEG with 20.0 PEG/PEI effectively protected particles from aggregation (154.5 ± 1.3 nm), but not the PEI–PEG with 11.1 PEG/PEI (634.6 ± 88.6 nm). With 0.1 mg/mL PEI, the size of the NPs was 215.2 ± 5.2 nm, whereas PEI–PEG coating gave NPs of 136.8 ± 6.1 nm and 175.1 ± 3.2 nm in the case of 20.0 and 11.1 PEG/PEI, respectively. The polydispersity indices for the NPs were similar at this concentration (0.23–0.27; Fig. 2B). The NP sizes did not change at the coating concentration of 0.3 mg/mL polymer ($p > 0.20$ by ANOVA). A typical AFM image (Fig. 3) for the 0.3 mg/mL PEI–PEG (20.0 PEG/PEI) coated NPs indicated spherical particles with 100–180 nm in size.

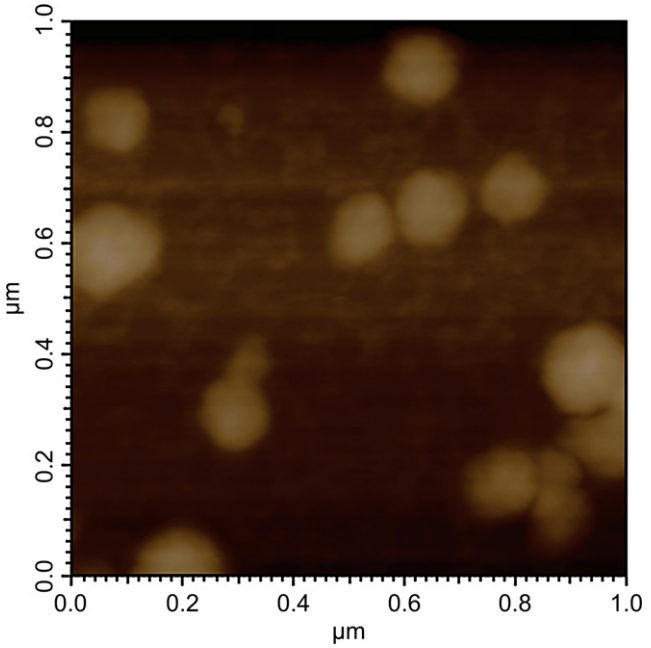

Fig. 3. The AFM image of PEI–PEG (20.0 PEG/PEI) coated NPs. The polymer concentration used for coating was 0.3 mg/mL. Distinct, relatively-uniform spherical particles were evident in the AFM image, with some particles displaying tails.

The zeta potential of the coated NPs increased from −16 mV to >10 mV (Fig. 2C). At 0.3 mg/mL, PEI coating produced the highest zeta potential among all the groups (29.7 mV) while the zeta potential of PEI–PEG coated NPs were 25.2 and 18.6 mV with 11.1 and 20.0 PEG/PEI coating, respectively ($p < 0.001$ by ANOVA). The reduction in zeta potential was consistent with the reduced cationic nature of PEI–PEG, as compared with PEI, used for NP coating.

The amount of polymer adsorbed onto NPs was determined by employing FITC-labeled polymers for coating (Fig. 4A). As the polymer concentration was increased, the amount of PEI adsorbed was clearly increased, unlike the PEI–PEG coating that showed relatively small increase with increasing polymer concentration. PEI–PEG coating resulted in 2.5–5.2 fold lower polymer coating as compared with the amount of PEI adsorbed onto the NP surfaces. The coating efficiency of polymers was dependent on the polymer concentration (Fig. 4B), significantly decreasing as the polymer

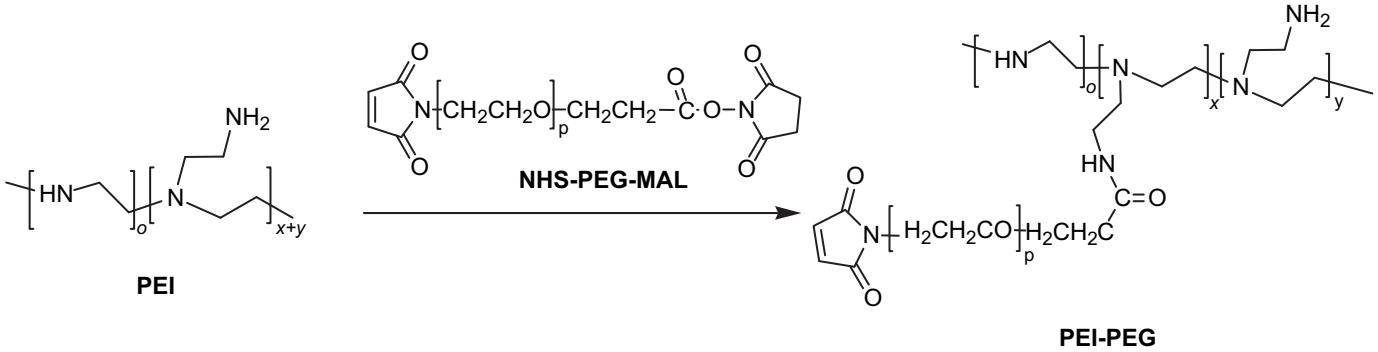

Scheme 1. Reaction scheme for NHS-PEG-MAL substitution on PEI. PEG segment was linked to the PEI backbone after the reaction of NHS functional group with primary amine to yield an amide linkage.

concentration used for coating was increased. The PEI demonstrated higher coating efficiency than the PEI–PEG polymers at the coating concentrations employed.

3.3. Cytotoxicity of polymer-coated NPs

The cytotoxicity of the PEI and PEI–PEG coated NPs on C2C12 cells are shown in Fig. 5. The polymer concentrations tested for NP coating were 0, 0.03, 0.1 and 0.3 mg/mL and different volumes of resultant NP suspensions (50, 25, 12.5 and 6.25 μL) were incubated with C2C12 cells. The results showed that the PEI–PEG coated NPs exhibited significantly reduced toxicity compared with the PEI-coated NPs at 50 μL of NP suspensions of 0.3 mg/mL polymer coating ($p < 0.001$): ~7% cell viability was obtained for NPs coated with PEI, while ~12% and ~45% cell viability was obtained for NPs coated with 11.1 and 20.0 PEG/PEI polymers, respectively. No significant difference in toxicity was observed for NPs when NP suspensions were ≤12.5 μL at 0.3 mg/mL polymer coating, with

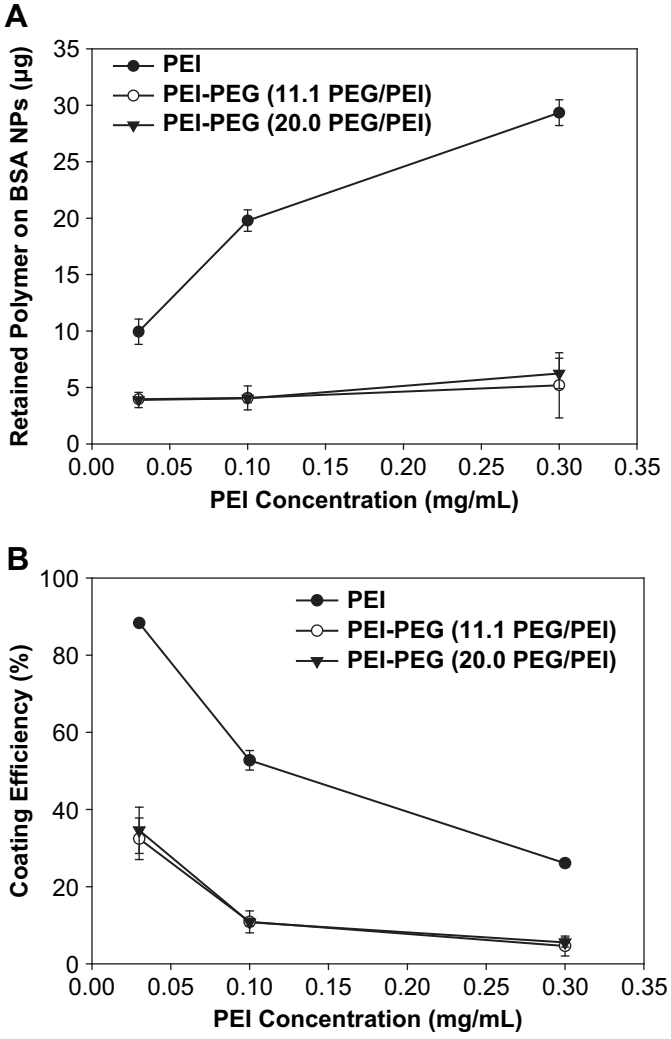

Fig. 4. (**A**) Amount of polymer coating on BSA NPs, as measured by adsorption of FITC-labeled polymers to the NPs ($n = 2$). The PEG was conjugated to FITC-PEI at different concentrations (1 and 3 mM) and the fluorescence adsorbed was measured as a function of polymer concentration, and then converted to mass (μg) of polymer adsorbed based on a calibration curve. The PEI amount adsorbed on the NPs was increased with the PEI concentration, while PEI–PEGs showed a small increase in adsorption as a function of polymer concentrations. (**B**) The efficiency of polymer coating was decreased as the polymer concentration increased, with the PEI giving the highest coating efficiency and PEI-PEG conjugates displaying lower coating efficiencies.

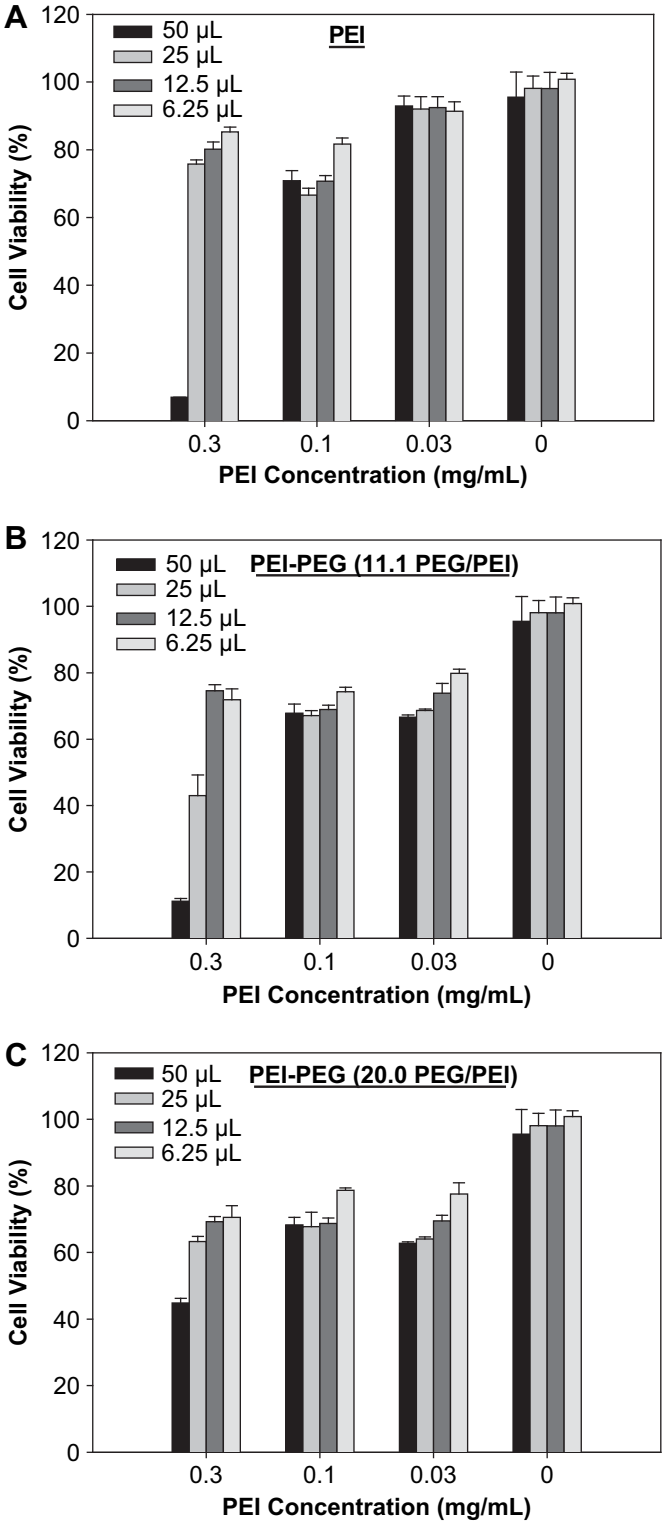

Fig. 5. Cytotoxicity of polymer-coated BSA NPs. The PEI-coated NPs (**A**) and two PEI–PEG coated NPs with 11.1 and 20.0 PEG/PEI (**B** and **C**, respectively) were assessed after coating at 0, 0.03, 0.1 and 0.3 mg/mL. Different volumes of NP suspensions (6.25, 12.5, 25, and 50 μL) were incubated with C2C12 cells for toxicity assessment. At the highest coating concentration (0.3 mg/mL), the PEI–PEG coated NPs demonstrated significantly reduced toxicity than the PEI-coated NPs at 50 μL of NP suspensions ($p < 0.001$). There was ≥70% cell viability at other coating concentrations with no apparent differences among different NPs.

≥70% cell viability for all polymers coating. At 0.1 and 0.03 mg/mL polymer coating, there was no significant difference in cell viability between the NPs coated with PEI and PEI–PEG at the NP volumes evaluated, with ≥70% cell viability demonstrated by all preparations. These results suggested that PEI–PEG coating reduced the cytotoxicity of coated NPs when polymer concentration for coating was higher than 0.1 mg/mL.

3.4. In vitro bioactivity of BMP-2 encapsulated in NPs

The ALP induction activities of BMP-2 encapsulated in the polymer-coated NPs are shown in Fig. 6. As in toxicity studies, the polymer concentrations employed for NP coating were 0, 0.03, 0.1 and 0.3 mg/mL and 50, 25, 12.5 and 6.25 μL of NP suspensions were incubated with human C2C12 cells. The results showed that at 0.3 mg/mL polymer coating, no ALP activity was observed for unmodified PEI at all NP volumes tested, while significant ALP activity was observed for PEI–PEG (11.1 PEG/PEI) at 12.5 and 6.25 μL of NP suspensions. Some ALP activity was exhibited for PEI–PEG (20.0 PEG/PEI) coated NPs even with 50 μL of NP suspension tested. This was consistent with the cytotoxicity result, where PEG substitution resulted in reduced toxicity. The PEI–PEG coated NPs generally possessed much higher ALP activity than PEI-coated NPs under the same conditions tested, except a nearly comparable ALP activity was seen for PEI and PEI–PEG coating at 0.1 mg/mL polymer concentration. The uncoated NPs showed relatively low ALP activity in this study, which was likely to represent BMP-2 loss from the unstable particles during the dialysis process.

3.5. NP implantation and in vivo ectopic bone formation

Prior to the subcutaneous implantation of BMP-2 containing NPs, the toxicity and ALP induction by the NP formulations were determined *in vitro* (Fig. 7). Since an unacceptable level of toxicity was seen with 0.3 mg/mL polymer coating and large aggregates were observed at 0.03 mg/mL polymer coating, the NPs for implantation were prepared at 0.1 mg/mL polymer coating concentration. No cell death was observed under microscope after polymer-coated NPs were incubated with human C2C12 cells for 48 h. The MTT results showed that the uncoated NPs and 0.1 mg/mL PEI-coated NPs demonstrated 100–140% cell viability depending on the volume of NP suspension added, and PEI–PEG coated NPs showed >80% cell viability at the highest volume of NP suspension added (Fig. 7A). The observed increase in cell viability could be due to increased cell numbers during the 48 h incubation period, and/or increased mitochondrial succinate dehydrogenase activity upon NP treatment. A dose-respondent ALP activity was observed for all groups tested, and PEI–PEG coated NPs exhibited the highest ALP activity, while PEI-coated NPs showed the lowest ALP activity among all the groups (Fig. 7B).

The wet weights of the implants recovered on days 10 and 16 were similar among the study groups on each day, albeit lower on day 16 by 20–40% (Fig. 8A). In order to compensate for the variations in explant weights, the ALP activity and calcium deposition were normalized against the weights. There was significant difference in ALP activity for the four study groups at both day 10 ($p < 0.013$) and day 16 ($p < 0.001$) (Fig. 8B). No evident ALP activity was shown in the control ACS group, while the uncoated NPs and PEI–PEG coated NPs demonstrated significant ALP activities at both day 10 and day 16. There was no significant difference in ALP activity between the PEI–PEG coated and uncoated NPs implants at both time points ($p > 0.63$ for day 10 and $p > 0.52$ for day 16). The implants loaded with PEI-coated NPs demonstrated marginal ALP activity, which was significantly lower than the PEI–PEG coated NPs on day 16 ($p < 0.01$).

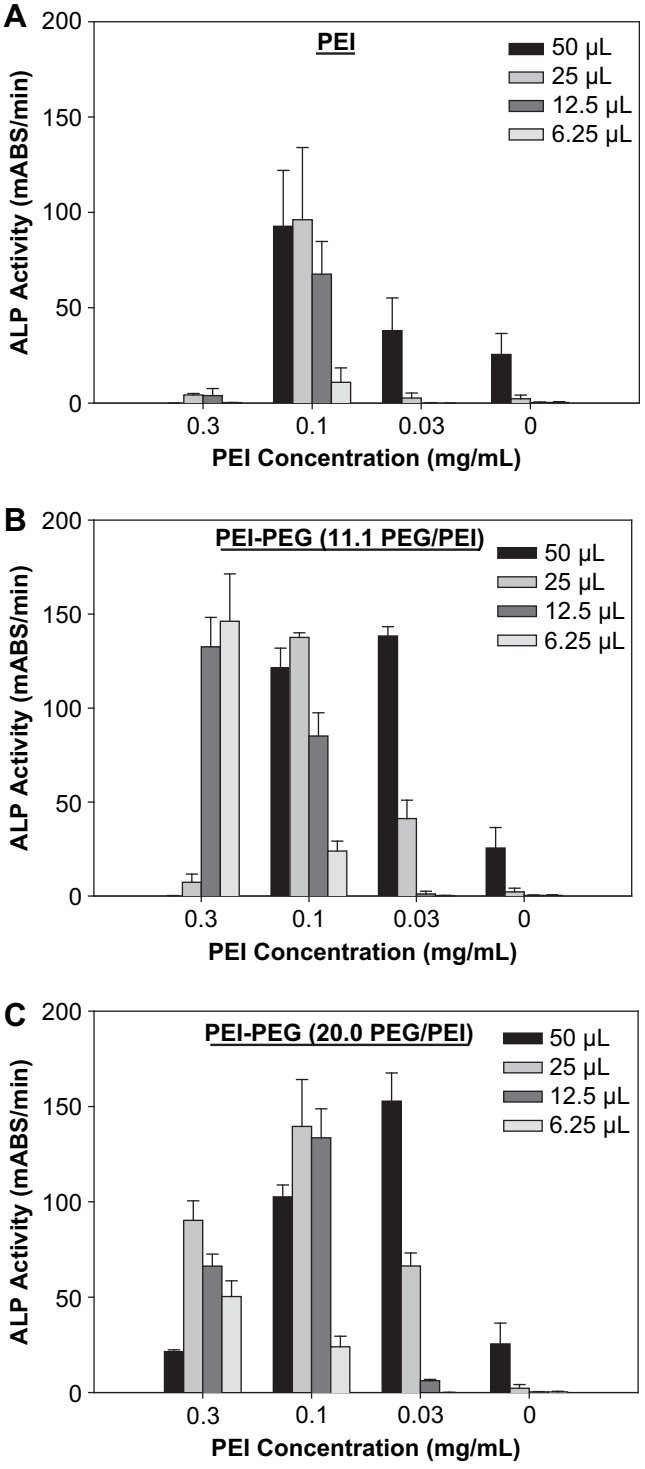

Fig. 6. The ALP induction by BMP-2 entrapped in PEI (**A**) and PEI–PEG (**B** and **C**) coated BSA NPs. The extent of PEG substitution was 11.1 and 20.0 PEG/PEI in B and C, respectively. The polymer coating concentrations tested were 0, 0.03, 0.1 and 0.3 mg/mL. Different volumes of the NP suspensions (6.25, 12.5, 25, and 50 μL) were incubated with C2C12 cells. The PEI–PEG coated NPs generally induced higher ALP activity than the PEI-coated NPs under the same conditions tested, except a nearly comparable ALP activity obtained at 0.1 mg/mL coating concentration.

There was significant difference in calcium deposition among the four study groups at both day 10 ($p < 0.05$) and day 16 ($p < 0.001$) (Fig. 8C). A significant increase in calcification from day 10 to day 16 was obtained for all three BMP-2 encapsulated

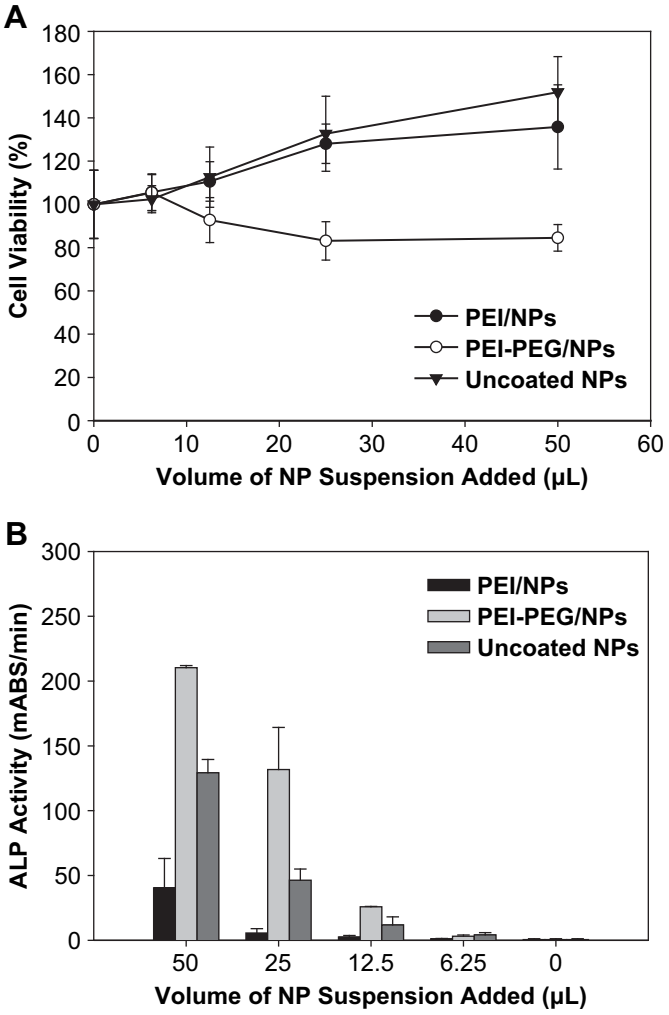

Fig. 7. *In vitro* assessment of cytotoxicity (**A**) and ALP induction (**B**) by the NPs used for implantation. There was no evident cytotoxicity exhibited by the three groups investigated, with >80% cell viability at all volumes examined. The PEI-PEG (20.0 PEG/PEI) coated NPs yielded the highest ALP activity among the three groups, and a dose-respondent ALP induction was observed for all groups.

NPs ($p < 0.004$). At day 16, calcification in the PEI–PEG coated NPs implant was the highest among all the groups, with a significant difference from the control and PEI-coated NPs implants ($p < 0.004$), but not from the uncoated NPs implant ($p > 0.42$). Note that a significant calcification was achieved by the PEI-coated NPs at day 16 compared with the control ($p < 0.004$). The correlation between the ALP activity and calcium deposition was significant at day 16 ($p < 0.0001$, by 2-tailed Pearson correlation), but did not reach to a significant level at day 10 ($p > 0.05$) (Fig. 8D).

The micro-CT images for all the recovered implants at day 10 and day 16 are shown in Fig. 9A and B, respectively. There was no evidence of bone formation in the control group at both time points. At day 10, the uncoated NPs induced new bone formation first as compared with other groups where sporadic calcification in PEI–PEG coated NPs was observed. However, at day 16, PEI–PEG coated NPs produced more extensive bone formation than the uncoated NPs, while the PEI-coated NPs resulted in relatively less bone formation. The deposited bone volume (mm^3), based on the quantitation of micro-CT images, mirrored the results of the calcification assay with similar non-parametric statistical results.

3.6. Pharmacokinetics analysis

The local retention of the implanted BMP-2 in different NP groups during a 7-day study period is summarized in Fig. 10. There was a gradual loss of BMP-2 from the implants in the 7 days post-implantation for all study groups. The BMP-2 encapsulated in PEI-coated NPs retained the highest amount of BMP-2 at day 1, as well as the subsequent time points ($p < 0.05$ vs. uncoated and PEI–PEG (20.0 PEG/PEI) coated NPs implants; ANOVA). There was no significant difference in BMP-2 retention between the uncoated NPs and the NPs coated with PEI–PEG (20.0 PEG/PEI) at all time points tested.

4. Discussion

As a critical growth factor in bone formation and healing, BMP-2 has been extensively studied and carriers made from different materials and geometries were employed for its delivery [40–42]. The main role of a delivery system for local bone induction is to retain the growth factor at the site of implantation for a prolonged time period, and protect the integrity of BMP-2 against interstitial proteases. In order to overcome the initial burst release and consequently low retention of BMP-2, we previously reported BMP-2 entrapment in PEI-coated BSA NPs, where the release of BMP-2 was controlled by a PEI coating layer [24]. However, the PEI-coated BMP-2/BSA NPs failed to elicit a robust bone formation when implanted in the rat ectopic model. The most likely reason for this observation was the cytotoxicity of PEI coating, which consequently abolished the ability of BMP-2 to exert its osteoinductive activity on target cells [28]. In this report, we aimed to design more biocompatible NPs by developing a new coating approach based on PEGylated PEI.

The ample primary amines in PEI facilitated the introduction of PEG onto PEI and the NHS moiety in NHS-PEG-MAL ensured a conjugate with stable amide linkages. Moreover, the MAL group, if desired, could be further modified with functional groups, for example, with cell-specific peptides or bisphosphonates for mineral affinity [32]. The MAL modification was not attempted in this study. Less than 25% of PEI amines were modified with PEG in this study. This was based on the concern of polymer coating onto BSA NPs afterwards, since PEGylation was expected to weaken the polyelectrolyte interactions between cationic polymer and the BSA NPs as a result of lower charge density and the increased hydrodynamic PEG layer [31]. As expected, PEGylated PEI, either in its soluble polymeric form or as part of the NP coating, demonstrated reduced cytotoxicity as compared with the unmodified PEI. This was the case when PEI–PEG was incubated with different cell lines in independent studies as well [43,44]. Furthermore, PEI–PEG coating influenced the physicochemical property of the resultant NPs. The size and zeta potential were significantly reduced after PEI–PEG coating, consistent with other reports when PEI–PEG was utilized to form polynucleotide complexes [43–46]. Note that the particle formation in the latter cases was driven by polyelectrolyte complexation via electrostatic interactions. The PEG modification minimized the aggregation of such complexes due to the increased hydrophilicity of the particles. A similar mechanism was expected to be responsible for the reduced NP sizes obtained with PEI–PEG coating as a result of preventing particle aggregation. Coating efficiency with PEI–PEG was significantly lower than the PEI, resulting in lower zeta potential of the PEI–PEG coated NPs. Owing to the dramatically reduced size and zeta potential, PEG-decorated BSA NPs might also hold the potential of intravascular injection, since such NPs are also expected to display the desirable "stealth" properties (i.e., reduced reticuloendothelial system uptake and prolonged circulation time) [47–49].

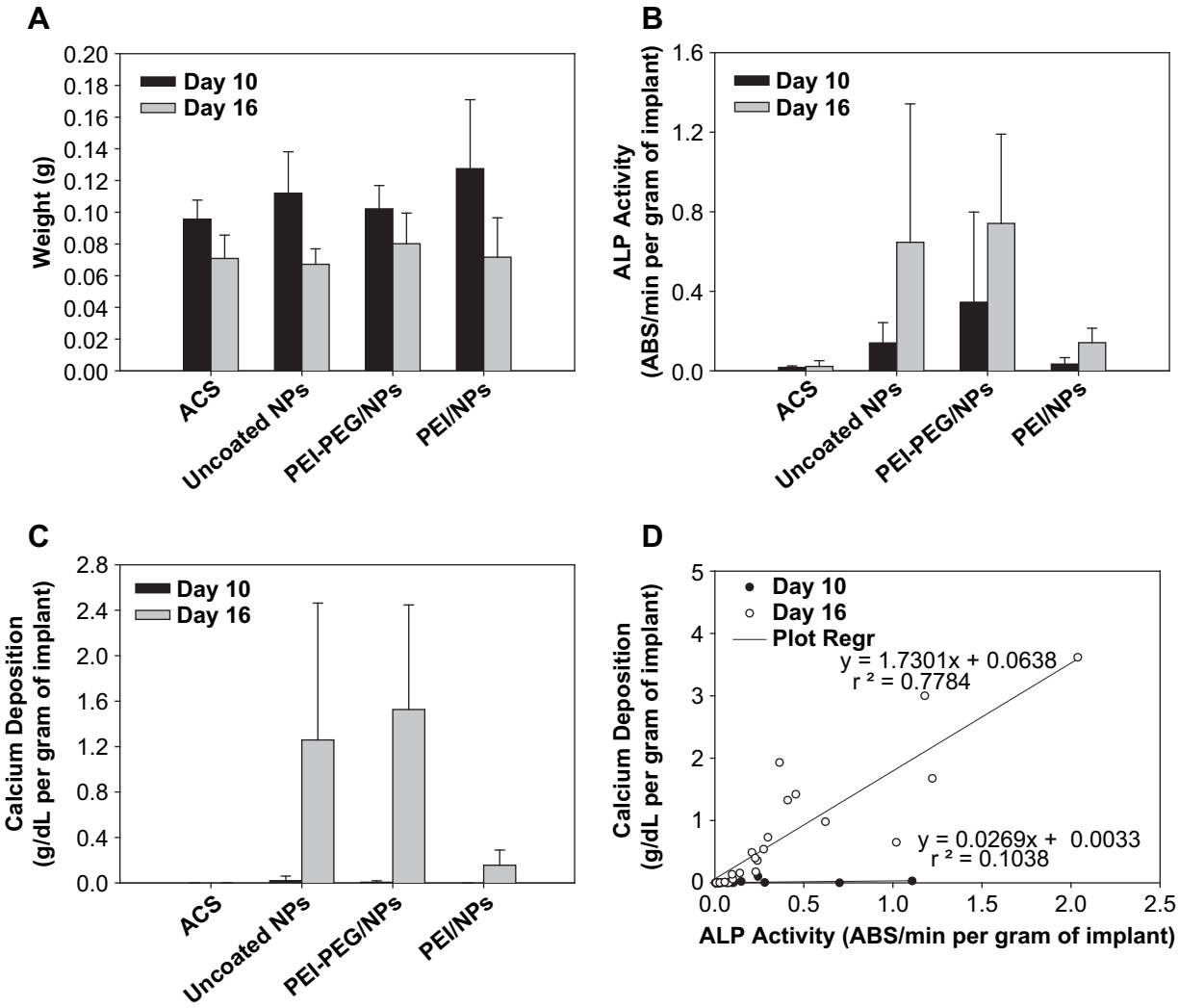

Fig. 8. *In vivo* osteoinductive effect of BMP-2 entrapped in BSA NPs. In all study groups, the amount of BMP-2 implanted was 3 μg except the control ACS group that had no BMP-2. The PEI–PEG coated NPs employed a polymer with 20.0 PEG/PEI. (**A**) Wet weight of recovered implants at day 10 and day 16; (**B**) Normalized ALP activity for the study groups at day 10 and day 16; (**C**) Normalized calcium deposition for the study groups at day 10 and day 16; and (**D**) Correlation between the calcium deposition and ALP activity of the recovered implants at day 10 and day 16. Note that a robust ALP induction and calcification was evident on day 16 in groups receiving uncoated and PEI–PEG coated NPs.

The BMP-2 is able to stimulate both ectopic and orthotopic bone regeneration as a result of local administration of the growth factor. In this study, we chose to load BMP-2 encapsulated NPs into ACS for the osteoinduction study. The ACS is one of the most extensively studied BMP-2 carriers, with the appropriate porous structure that allows vascularization and bone deposition. However, the control over release kinetics was limited and initial burst release of BMP-2 is an inherent problem associated with this carrier, since BMP-2 is simply adsorbed into ACS for implantation [50,51]. By loading ACS with BMP-2 encapsulated NPs, the NP formulation has the potential to control the BMP-2 release and possibly reduce the initial burst release of BMP-2. This was shown to be the case with the PEI-coated NPs and it is likely that the high cationic surface of the NPs helped to facilitate the NP binding to ACS and to prolong its retention locally. NPs coated with PEI–PEG seemingly did not reduce the initial burst of BMP-2, possibly due to the reduced interactions of NP with the ACS scaffold.

In the implantation study, 0.1 mg/mL polymer concentration was chosen to coat the NPs as NPs coated at this concentration demonstrated little toxicity and high ALP activity *in vitro*. The BMP-2 loading in NPs was increased as compared to our previous study (9.6% vs. 1.44% w/w [28]), so that a desired BMP-2 implant dose could be achieved without the need for NP 'concentration' that was attempted before [28]. The beneficial effect of the PEI–PEG coating was obvious in this assay. In addition to the improved biocompatibility of PEGylated PEI, which caused less toxicity in the surrounding tissue, it is likely that smaller BSA NPs and a weaker PEI–PEG coating on NPs might have led to faster BMP-2 release locally. Our pharmacokinetics data did not reveal a gross difference between the uncoated NPs and PEI–PEG coated NPs in BMP-2 release *in situ*, but it is probable that the difference might exist within the scaffolds, which are not readily revealed by measuring the total amount of BMP-2 in the recovered implants. Others showed that it was possible to achieve NP modification with PEG without affecting the release pattern of the drugs, as suggested by one study on drug delivery to brain with albumin NPs [52]. This was also implied by the PEI–PEG coated NPs, which yielded higher ALP activity and more extensively calcium deposition than the uncoated NPs at day 16.

It is difficult to compare the efficacy of different carriers for BMP-2 delivery due to the variations in carrier geometries, BMP-2 loadings, animal species, ages and implantation sites, as well as the explantation times reported in literatures [53]. Similar approach by using NPs for BMP-2 delivery was conducted by Chung et al. [27],

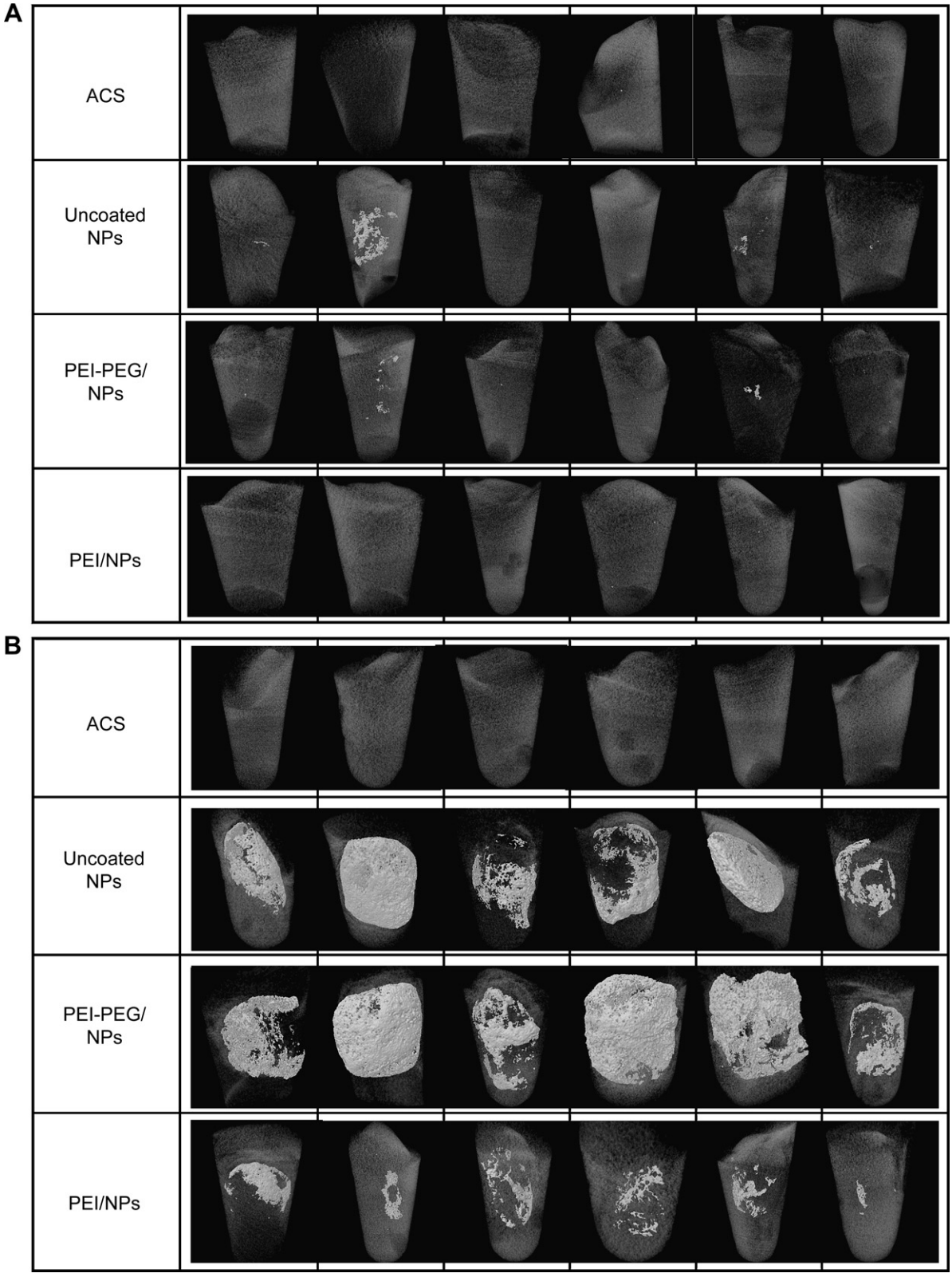

Fig. 9. Micro-CT images of the implants recovered on 10 (**A**) and 16 (**B**) days post-implantation. Individual implants were shown in each study group. Calcification was most evident on day 16 and for the groups receiving uncoated and PEI–PEG coated NPs. (**C**) The calculated bone volumes (mean ± SD) for the scanned images.

where the osteoinduction of BMP-2 loaded heparin-functionalized poly(D,L-lactic-co-glycolic acid) (PLGA) NPs in fibrin hydrogel was investigated in rat calvarial critical size defect model. Heparin was entrapped onto the surface of PLGA NPs for specific complexation with BMP-2, and then the BMP-2 loaded NPs were incorporated into fibrin gel. At week 4, significantly higher bone formation was found in the BMP-2 loaded NP-fibrin gel complex than the BMP-2 loaded fibrin gel without functionalized NPs, which suggested that

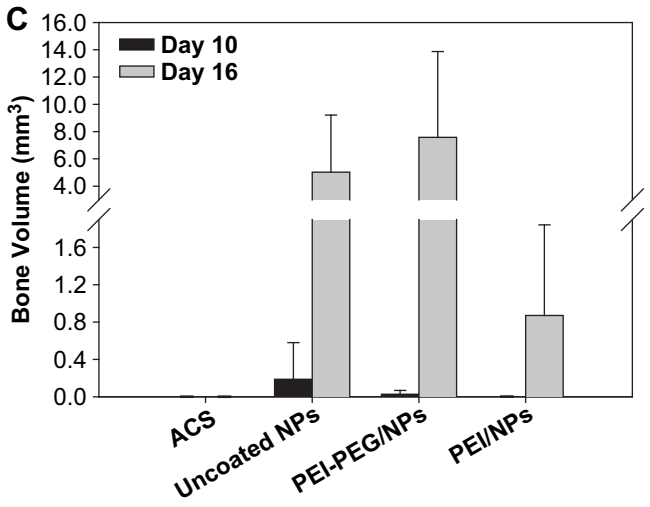

Fig. 9. (*Continued*).

a more controlled release of BMP-2 was achieved in the former carrier. Another study by Wei et al. investigated the bone regeneration of BMP-7 encapsulated PLGA nanospheres in poly(L-lactic acid) (PLLA) scaffold in rat ectopic model [54]. The BMP-7 containing nanosphere-PLLA scaffold induced significant bone formation while passive adsorption of BMP-7 solution into PLLA scaffold failed to generate bone at 6 weeks post-implantation. It was likely due to the nanosphere-scaffold delivery system released and localized BMP-7 for a desired duration at the implantation site, while simple adsorption of BMP-7 into the scaffold seemed to give a bolus or pulse release of BMP-7 with substantial loss of bioactivity, which led to the failure of new bone formation. Encapsulation of growth factors in NPs followed by combination with matrix or scaffold as hybrid carrier for bone regeneration has been demonstrated to be a successful strategy to achieve prolonged release of bioactive growth factors [27,54–56]. The growth factor release from the carriers can be tailored by the modification of NPs. This is also a versatile approach that can be expanded to many bioactive molecules.

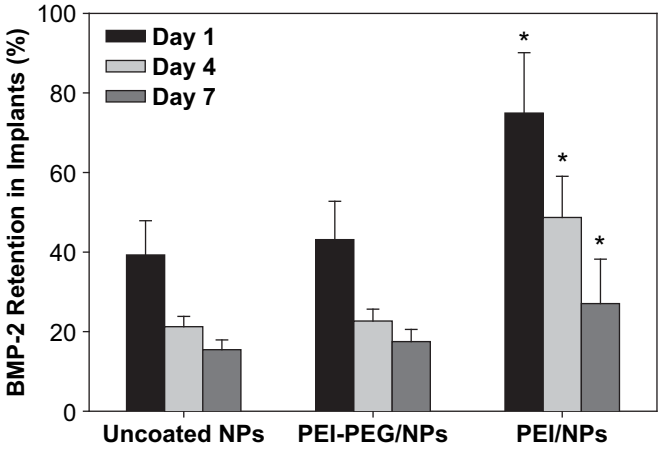

Fig. 10. Pharmacokinetics of BMP-2 in different BSA NP formulations in the rat ectopic implant model. The results were summarized as the percent retention of the implanted BMP-2 dose at three time points (days 1, 4, and 7). The PEI-coated BMP-2/BSA NPs gave significantly higher BMP-2 retention at all time points as compared with the uncoated BMP-2/BSA NPs and the PEI–PEG coated NPs ($p < 0.05$ by ANOVA). No apparent differences in BMP-2 retention were noted between the uncoated and PEI–PEG coated NPs.

It has been estimated that normal bone contains approximately 2 μg of BMP-2 per kilogram of pulverized bone [57]. Since BMP-2 has a very short half-life, ~7–16 min [58], in systemic circulation, and is rapidly degraded *in vivo*, a controlled and localized delivery system for a small amount of BMP-2 would be appropriate for effective bone regeneration. Currently the BMP-2 concentrations in use (micrograms to milligrams) are supraphysiological, compared with nanogram ranges of BMP-2 *in vivo* [57]. In addition to the danger of excess bone formation, possible overflow of BMP-2 from the implant may upregulate the BMP-2 inhibitors such as noggin or sclerotin, and interfere with the bone induction process [59]. The delivery system that releases BMP-2 at the appropriate dose and kinetics can be advantageous for the growth factor therapy, and NP formulations for this purpose have the potential to broadly benefit clinical bone repair.

5. Conclusions

In this study, PEG substitution was shown to effectively reduce the toxicity of PEI, and the PEI–PEG employed for BSA NP coating dramatically reduced the size and zeta potential of NPs, compared with the NPs coated with PEI. The higher PEG substitution on PEI displayed a more pronounced effect in the reduction of NP size and zeta potential. Effective bone formation in the rat ectopic model was achieved with the BMP-2 encapsulated in BSA NPs coated with 0.1 mg/mL PEI–PEG (20.0 PEG/PEI), as determined by the higher ALP activity and calcification in the recovered implants. The BMP-2/BSA NPs coated with 0.1 mg/mL PEI demonstrated less bone formation than the PEI–PEG coated NPs. The advantage of PEI–PEG coated BMP-2/BSA NPs for bone formation was attributed to the improved biocompatibility and physiochemical properties. Based on the performance of the designed effective NP formulation, this system can potentially benefit local bone regeneration as well as targeted bone stimulation after intravascular injection. The NP formulations of BMP-2 can be also combined with other matrices or scaffolds for application to large orthotopic defect sites.

Acknowledgements

The authors thank the technicians, Mr. Charles Tran and Ms. Jillian Chapman in the Pharmacy Micro-CT (PMCT) imaging laboratory (Faculty of Pharmacy and Pharmaceutical Sciences, University of Alberta), for their assistance with the micro-CT study. This project was financially supported by an operating grant from the Canadian Institutes of Health Research (CIHR). Infrastructure support was provided by Canadian Foundation for Innovation (CFI) and Alberta Heritage Foundation for Medical Research (AHFMR).

Appendix

Figures with essential colour discrimination. Certain figures in this article, in particular Fig. 3, may be difficult to interpret in black and white. The full colour images can be found in the on-line version, at doi:10.1016/j.biomaterials.2009.10.011.

References

[1] Bessa PC, Casal M, Reis RL. Bone morphogenetic proteins in tissue engineering: the road from laboratory to clinic, part II (BMP delivery). J Tissue Eng Regen Med 2008;2:81–96.
[2] Barboza EP, Duarte MEL, Geolas L, Sorensen RG, Riedel GE, Wikesjö UME. Ridge augmentation following implantation of recombinant human bone morphogenetic protein-2 in the dog. J Periodontol 2000;71:488–96.
[3] Boyne PJ. Application of bone morphogenetic proteins in the treatment of clinical oral and maxillofacial osseous defects. J Bone Joint Surg Am 2001;83:S146–50.

[4] Chen B, Lin H, Wang J, Zhao Y, Wang B, Zhao W, et al. Homogeneous osteogenesis and bone regeneration by demineralized bone matrix loading with collagen-targeting bone morphogenetic protein-2. Biomaterials 2007;28:1027–35.
[5] Levine J, Bradley J, Turk AE, Ricci JL, Benedict JJ, Steiner G, et al. Bone morphogenetic protein promotes vascularization and osteoinduction in pre-formed hydroxyapatite in the rabbit. Ann Plast Surg 1997;39:158–68.
[6] Ripamonti U, Ramoshebi LN, Matsaba T, Tasker J, Crooks J, Teare J. Bone induction by BMPs/OPs and related family members in primates: the critical role of delivery systems. J Bone Joint Surg Am 2001;83:S116–27.
[7] Sandhu HS, Khan SN. Animal models for preclinical assessment of bone morphogenetic proteins in the spine. Spine 2002;27:S32–8.
[8] Wozney JMP, Rosen VP. Bone morphogenetic protein and bone morphogenetic protein gene family in bone formation and repair. Clin Orthop Relat Res 1998;346:26–37.
[9] Boden SD, Zdeblick TA, Sandhu HS, Heim SE. The use of rhBMP-2 in interbody fusion cages. Spine 2000;25:376–81.
[10] Boden SD, Martin GJJ, Morone MA, Ugbo JL, Moskovitz PA. Posterolateral lumbar intertransverse process spine arthrodesis with recombinant human bone morphogenetic protein-2/hydroxyapatite-tricalcium phosphate after laminectomy in the nonhuman primate. Spine 1999;24:1179.
[11] Boden SD. Overview of the biology of lumbar spine fusion and principles for selecting a bone graft substitute. Spine 2002;27:S26–31.
[12] Baskin DS, Ryan P, Sonntag V, Westmark R, Widmayer M. A prospective, randomized, controlled cervical fusion study using recombinant human bone morphogenetic protein-2 with the CORNERSTONE-SR™ allograft ring and the ATLANTIS™ anterior cervical plate. Spine 2003;28:1219–24.
[13] Cook SD. Preclinical and clinical evaluation of osteogenic protein-1 (BMP-7) in bony sites. Orthopedics 1999;22:669–71.
[14] Friedlaender GE, Perry CR, Cole JD, Cook SD, Cierny G, Muschler GF, et al. Osteogenic protein-1 (bone morphogenetic protein-7) in the treatment of tibial nonunions – a prospective, randomized clinical trial comparing rhOP-1 with fresh bone autograft. J Bone Joint Surg Am 2001;83A:S151–8.
[15] Dinopoulos H, Giannoudis PV. The use of bone morphogenetic proteins (BMPs) in long-bone non-unions. Curr Orthop 2007;21:268–79.
[16] Wang EA. Bone morphogenetic proteins (BMPs): therapeutic potential in healing bony defects. Trends Biotechnol 1993;11:379–83.
[17] Sykaras N, Opperman LA. Bone morphogenetic proteins (BMPs): how do they function and what can they offer the clinician? J Oral Sci 2003;45:57–73.
[18] Uludağ H, D'Augusta D, Palmer R, Timony G, Wozney J. Characterization of rhBMP-2 pharmacokinetics implanted with biomaterial carriers in the rat ectopic model. J Biomed Mater Res 1999;46:193–202.
[19] Uludağ H, D'Augusta D, Golden J, Li J, Timony G, Riedel R, et al. Implantation of recombinant human bone morphogenetic proteins with biomaterial carriers: a correlation between protein pharmacokinetics and osteoinduction in the rat ectopic model. J Biomed Mater Res 2000;50:227–38.
[20] Uludağ H, Gao T, Porter TJ, Friess W, Wozney JM. Delivery systems for BMPs: factors contributing to protein retention at an application site. J Bone Joint Surg Am 2001;83:S128–35.
[21] Lane JM. BMPs: why are they not in everyday use? J Bone Joint Surg Am 2001;83:S161–2.
[22] Luginbuehl V, Meinel L, Merkle HP, Gander B. Localized delivery of growth factors for bone repair. Eur J Pharm Biopharm 2004;58:197–208.
[23] Kim SE, Jeon O, Lee JB, Bae MS, Chun HJ, Moon SH, et al. Enhancement of ectopic bone formation by bone morphogenetic protein-2 delivery using heparin-conjugated PLGA nanoparticles with transplantation of bone marrow-derived mesenchymal stem cells. J Biomed Sci 2008;15:771–7.
[24] Zhang S, Wang G, Lin X, Chatzinikolaidou M, Jennissen H, Laub M, et al. Polyethylenimine-coated albumin nanoparticles for BMP-2 delivery. Biotechnol Prog 2008;24:945–56.
[25] Wang G, Siggers K, Zhang S, Jiang H, Xu Z, Zernicke RF, et al. Preparation of BMP-2 containing bovine serum albumin (BSA) nanoparticles stabilized by polymer coating. Pharm Res 2008;25:2896–909.
[26] Yigor P, Tuzlakoglu K, Reis RL, Hasirci N, Hasirci V. Incorporation of a sequential BMP-2/BMP-7 delivery system into chitosan-based scaffolds for bone tissue engineering. Biomaterials 2009;30:3551–9.
[27] Chung YI, Ahn KM, Jeon SH, Lee SY, Lee JH, Tae G. Enhanced bone regeneration with BMP-2 loaded functional nanoparticle-hydrogel complex. J Control Release 2007;121:91–9.
[28] Zhang S, Doschak MR, Uludağ H. Pharmacokinetics and bone formation by BMP-2 entrapped in polyethylenimine-coated albumin nanoparticles. Biomaterials 2009;30:5143–55.
[29] Pathak Y, Thassu D, Deleers M. Pharmaceutical applications of nanoparticulate drug-delivery systems. In: Thassu D, Deleers M, Pathak Y, editors. Nanoparticulate drug delivery systems. New York: Informa Healthcare; 2007. p. 185–212.
[30] Hermanson GT. Modification with synthetic polymers. In: Bioconjugate techniques. San Diego: Academic Press; 1996. p. 605–29.
[31] Hinds KD. Protein conjugation, cross-linking and PEGylation. In: Mahato RI, editor. Biomaterials for delivery and targeting of proteins and nucleic acids. Boca Raton: CRC Press; 2005. p. 120–88.
[32] Zhang S, Wright JEI, Özber N, Uludağ H. The interaction of cationic polymers and their bisphosphonate derivatives with hydroxyapatite. Macromol Biosci 2007;7:656–70.
[33] Ruppert R, Hoffmann E, Sebald W. Human bone morphogenetic protein 2 contains a heparin-binding site which modifies its biological activity. Eur J Biochem 1996;237:295–302.
[34] Perrine TD, Landis WR. Analysis of polyethylenimine by spectrophotometry of its copper chelate. J Polym Sci 1967;5:1993–2003.
[35] Von Harpe A, Petersen H, Li Y, Kissel T. Characterization of commercially available and synthesized polyethylenimines for gene delivery. J Control Release 2000;69:309–22.
[36] Bullock J, Chowdhury S, Severdia A, Sweeney J, Johnston D, Pachla L. Comparison of results of various methods used to determine the extent of modification of methoxy polyethylene glycol 5000-modified bovine cuprizinc superoxide dismutase. Anal Biochem 1997;254:254–62.
[37] Gittens SA, Bansal G, Kucharski C, Borden M, Uludağ H. Imparting mineral affinity to fetuin by bisphosphonate conjugation: a comparison of three bisphosphonate conjugation schemes. Mol Pharm 2005;2:392–406.
[38] Varkey M, Kucharski C, Haque T, Sebald W, Uludağ H. *In vitro* osteogenic response of rat bone marrow cells to bFGF and BMP-2 treatments. Clin Orthop Relat Res 2006;443:113–23.
[39] Hiemenz PC, Rajagopalan R. Electrostatic and polymer-induced colloid stability. In: Principles of colloid and surface chemistry. 3rd ed. New York: Marcel Dekker; 1997. p. 604–10.
[40] Winn SR, Uludağ H, Hollinger JO. Carrier systems for bone morphogenetic proteins. Clin Orthop Relat Res 1999;367:S95–106.
[41] LeGeros RZ. Properties of osteoconductive biomaterials: calcium phosphates. Clin Orthop Relat Res 2002;395:81–98.
[42] Baldwin SP, Saltzman WM. Materials for protein delivery in tissue engineering. Adv Drug Deliv Rev 1998;33:71–86.
[43] Petersen H, Fechner PM, Martin AL, Kunath K, Stolnik S, Roberts CJ, et al. Polyethylenimine-graft-poly(ethylene glycol) copolymers: influence of copolymer block structure on DNA complexation and biological activities as gene delivery system. Bioconjug Chem 2002;13:845–54.
[44] Tang GP, Zeng JM, Gao SJ, Ma YX, Shi L, Li Y, et al. Polyethylene glycol modified polyethylenimine for improved CNS gene transfer: effects of PEGylation extent. Biomaterials 2003;24:2351–62.
[45] Kunath K, Von Harpe A, Petersen H, Fischer D, Voigt K, Kissel T, et al. The structure of PEG-modified poly(ethylene imines) influences biodistribution and pharmacokinetics of their complexes with NF-kB decoy in mice. Pharm Res 2002;19:810–7.
[46] Remaut K, Lucas B, Raemdonck K, Braeckmans K, Demeester J, De Smedt SC. Protection of oligonucleotides against enzymatic degradation by pegylated and nonpegylated branched polyethyleneimine. Biomacromolecules 2007;8:1333–40.
[47] Niidome T, Yamagata M, Okamoto Y, Akiyama Y, Takahashi H, Kawano T, et al. PEG-modified gold nanorods with a stealth character for *in vivo* applications. J Control Release 2006;114:343–7.
[48] Bazile D, Prud'homme C, Bassoullet MT, Marlard M, Spenlehauer G, Veillard M, et al. PEG–PLA nanoparticles avoid uptake by the mononuclear phagocytes system. J Pharm Sci 1995;84:493–8.
[49] Waku T, Matsusaki M, Kaneko T, Akashi M. PEG brush peptide nanospheres with stealth properties and chemical functionality. Macromolecules 2007;40:6385–92.
[50] Helm GA, Sheehan JM, Sheehan JP, Jane JA, Dipierro CG, Simmons NE, et al. Utilization of type I collagen gel, demineralized bone matrix, and bone morphogenetic protein-2 to enhance autologous bone lumbar spinal fusion. J Neurosurg 1997;86:93–100.
[51] Takahashi Y, Yamamoto M, Tabata Y. Enhanced osteoinduction by controlled release of bone morphogenetic protein-2 from biodegradable sponge composed of gelatin and β-tricalcium phosphate. Biomaterials 2005;26:4856–65.
[52] Mishra V, Mahor S, Rawat A, Gupta PN, Dubey P, Khatri K, et al. Targeted brain delivery of AZT via transferrin anchored pegylated albumin nanoparticles. J Drug Target 2006;14:45–53.
[53] Winn SR, Uludağ H, Hollinger JO. Sustained release emphasizing recombinant human bone morphogenetic protein-2. Adv Drug Deliv Rev 1998;31:303–18.
[54] Wei G, Jin Q, Giannobile WV, Ma PX. The enhancement of osteogenesis by nano-fibrous scaffolds incorporating rhBMP-7 nanospheres. Biomaterials 2007;28:2087–96.
[55] Chen FM, Zhao YM, Zhang R, Jin T, Sun HH, Wu ZF, et al. Periodontal regeneration using novel glycidyl methacrylated dextran (Dex-GMA)/gelatin scaffolds containing microspheres loaded with bone morphogenetic proteins. J Control Release 2007;121:81–90.
[56] Fan H, Hu Y, Qin L, Li X, Wu H, Lv R. Porous gelatin–chondroitin–hyaluronate tri-copolymer scaffold containing microspheres loaded with TGF-beta1 induces differentiation of mesenchymal stem cells *in vivo* for enhancing cartilage repair. J Biomed Mater Res 2006;77A:785–94.
[57] Rengachary SS. Bone morphogenetic proteins: basic concepts. Neurosurg Focus 2002;13:1–6.
[58] Zhao B, Katagiri T, Toyoda H, Takada T, Yanai T, Fukuda T, et al. Heparin potentiates the *in vivo* ectopic bone formation induced by bone morphogenetic protein-2. J Biol Chem 2006;281:23246–53.
[59] Westerhuis RJ, Van Bezooijen RL, Klloen P. Use of bone morphogenetic proteins in traumatology. Injury 2005;36:1405–12.